







# PRODUCTION ENGINEERING ARCHIVES

ISSN 2353-5156 (print)  
ISSN 2353-7779 (online)

Exist since 4<sup>th</sup> quarter 2013  
Available online at <https://pea-journal.eu>

## Development and Performance Evaluation of a Pulverizer for Plantain Flour Process Plant

Emmanuel Olatunji Olutomilola<sup>1</sup>, Sesan Peter Ayodeji<sup>1</sup>, Michael Kanisuru Adeyeri<sup>1</sup>, Tayo Nathaniel Fagbemi<sup>2</sup>

<sup>1</sup> Industrial and Production Engineering Department/Mechanical Engineering Department, School of Engineering and Engineering Technology, Federal University of Technology, P.M.B 704, Akure, 340271, Ondo State, Nigeria

<sup>2</sup> Food Science Technology Department, School of Agriculture and Agricultural Technology, Federal University of Technology, P.M.B 704, Akure, 340271, Ondo State, Nigeria

Corresponding author e-mail: [oolutomilola@futa.edu.ng](mailto:oolutomilola@futa.edu.ng)

### Article history

Received 14.05.2021  
Accepted 29.07.2021  
Available online 06.09.2021

### Keywords

Diabetes COVID-19  
Pulverizer development  
Performance evaluation  
Plantain  
Flour process plant

### Abstract

Diabetes, adjudged a risk factor for coronavirus infectious disease 2019 (COVID-19), can be managed through consumption of plantain and its associated products. Plantain is usually processed into flour and other storable/value-added products due to its very short shelf-life. To process unripe plantain pulps into flour, there is a need for size reduction after drying. This paper presents the development and performance evaluation of a size reduction unit for pulverizing, sieving and conveying material to the next processing stage in a plantain flour process plant. Its model was developed using solidworks application software. After design analysis, the model was simulated to establish its suitability/adequacy for fabrication. The pulverizer was fabricated using locally available materials. Its performance evaluation gave 400kg/h throughput, 96% crushing efficiency and 96% efficiency based on the required particle size. The average particle size of flour obtained was 236 $\mu$ m using 500 $\mu$ m screen. Effect of cyclone control-valve on the pulverizer's overall efficiency was also investigated by allowing it to operate when the valve was completely closed, partially closed and fully opened. It was observed that the control-valve's positions significantly influenced the machine's performance/efficiency. It can thus be inferred that the position of cyclone control-valve has significant effect on a pulverizer's efficiency/performance. Hence, leaving control-valve fully opened during operation would help a pulverizer perform with optimum efficiency, as the pulverizer was able to convey material, efficiently in that position, to the next processing stage during performance evaluation.

DOI: 10.30657/pea.2021.27.30

JEL: Q16, Q30, O13, L66

## 1. Introduction

The management of diabetes without negative side effects is said to be a challenge in the world (Ajiboye et al., 2018; Olutomilola, 2021). Diabetes, adjudged a risk factor for COVID-19 (Seewoodhary and Oozageer, 2020; Adeyeri et al., 2020), has been associated with worse outcomes in COVID-19 patients (Hussain et al., 2020). Its presence is also associated with increased mortality among COVID-19 patients (Olutomilola et al., 2019; Wang et al., 2020). Diabetes is said to be among the five leading causes of deaths and debilitating diseases on earth (Oluwajuyitan and Ijarotimi, 2019). However, plantain is found to be very effective and affordable for managing diabetes mellitus without adverse side effects (Oluwajuyitan and Ijarotimi, 2019; Olutomilola et al., 2020).

Consumption of plantain and its associated products seems to be one of the promising ways to weaken and win the war against COVID-19, following the recommendation of unripe plantain flour for dietary management of diabetes mellitus (Olutomilola, 2021). The quest to manage diabetes mellitus and mitigate the alarming postharvest losses of plantain in Nigeria (the fifth largest producer of plantain in the world) gave birth to this research work. The study shows that postharvest losses of plantain usually range from 5% to over 50% in Nigeria (Morris et al., 2019; Olutomilola et al., 2021; Olutomilola, 2021). Plantain is usually processed into flour and other storable or value-added products due to its perishable nature and to ease transportation from one location to another for commercial purposes (Olutomilola and Omoaka, 2018; Olutomilola et al., 2020). The alarming postharvest losses of

plantain, increasing market demand for plantain and its by-products, and being the fourth most important crop on earth (Olutomilola et al., 2021; Alonso-Gomez et al., 2020), necessitated that a plant be developed in Nigeria for processing the crop into flour (Ayodeji, 2016). The process plant should consist of different units that will handle all the processes involved in processing unripe plantain into flour, one of which is a size reduction or pulverizing unit.

There are different size reduction methods for dry solid food materials: disc or bur mill, ball mill, hammer mill and roller mill. In all of these size reduction methods, there are three types of forces that are used to effect size reduction of food materials: compression, impact and shearing (or attrition) forces. It is a known fact that hammer mills, due to their high throughput rates and ability to grind different materials, are the most widely used size reduction equipment for dry materials (Probst et al., 2013). Hammer mill consists of a feed inlet (which is arranged so that the operator cannot put his hand inside the hammer mill), a horizontal cylindrical chamber, a high-speed rotor, an electric motor and a belt drive. According to Kock (2002) and Fenchea (2012), rotor usually consists of a main shaft, three disks (which are mounted on the main shaft), pin shafts (which run parallel to the main shaft and through the rotor) and free-swinging hammers (known as beaters) or fixed hammers, which are suspended from the pin shafts.

## 2. Literature review

Many researchers have developed hammer mills which can be adopted for milling dry plantain pulps in a plantain flour production and packaging plant. Nasir (2005) developed a hammer mill from locally available materials for grinding dry farm produce, which had a crushing efficiency of 96% and a crushing capacity of 31 kg/hr. Ebunilo et al. (2010) developed a hammer mill with end-suction lift capability for processing grains and minerals. Jibrin et al. (2013) developed a hammer mill for crushing crop residues for the purpose of animal feed. Ogedengbe and Abadariki (2014) developed a hammer mill for pulverizing animal bone into bone-meal, which was able to pulverize at an average rate of 4.68 g/s. Adekomaya and Samuel (2014) developed a petrol-powered hammer mill for small scale industries and rural farmers in Nigeria, with a crushing efficiency of 94%. Ajaka and Adesina (2014) developed a laboratory size hammer mill from locally available materials for crushing minerals whose principle of operation can perfectly work for pulverizing dry plantain pulps. Adetola and Oyejide (2015) developed a hammer mill, with 86.9% crushing efficiency, for pulverizing cow bone which was incorporated with safety hollow for housing hard foreign materials that are different from bones. Mohamed et al. (2015) developed a hammer mill for crushing and pulverizing grains, rice straw, cotton straw and other materials, with a crushing efficiency of 94.7%. Moreover, Hadi et al. (2017) developed an improved hammer mill by redesigning the beaters, milling chamber shape and the shaft. The shaft was redesigned to allow incorporation of variable speed gasoline engine as a replacement for electric motor and an average

crushing efficiency of 92.47% was obtained. Hence, the design and principle of operation of the machines developed by these aforementioned researchers as well as the outcomes of their studies were very helpful in developing a pulverizer for the plantain processing plant. Despite the successes recorded by these aforementioned researchers, it is still necessary to develop a unit, using locally available materials (for easy maintenance and cost-effectiveness), which will be able to pulverize dried plantain pulp, sieve it and then convey it to the next processing stage in a plantain flour production and packaging plant. This is the goal of this research work.

## 3. Methods and materials

### 3.1. Description and operation of the pulverizer

The pulverizer is a gravity feed and pneumatic-gravity discharge type of hammer mill. Hammer mill was selected because of its high throughput rates and ability to grind different dry materials (Probst et al., 2013). It consists of a feed inlet or hopper, the milling chamber, a high-speed rotor, a 500 $\mu$ m screen or sieve, an electric motor, two v-belts, two pulleys, a belt safety-guard, supporting frame, suction-fan assembly, pipes and elbows, a cyclone, a control-valve for cyclone, two pillow block bearings, three baft bags, and cyclone stand as shown in Fig. 1. The rotor consists of a main shaft, four hammer mounting rods (which run parallel to the main shaft and through the rotor), three hammer mounting plates (which are mounted on the main shaft to help secure the hammer mounting rods), free-swinging hammers (known as beaters, which are suspended from the hammer mounting rods) and spacers. The hammer mounting rods are fitted into drilled-holes on the mounting plates. The pulverizer is driven by a 1460 rpm, one phase and 3.69 kW electric motor.

The dry plantain pulps to be pulverized are fed into the hopper and travel through the inlet housing into the milling chamber, where particle reduction takes place as a result of the centrifugal force impacted on them by the beaters. The pulverized pulps are screened out of the milling compartment through the outlet housing, where they are sucked and thrown through pipes into cyclone by the suction-fan – mounted on the main shaft outside the milling chamber. The uniqueness of this machine is in the fact that the suction-fan is also powered by the main shaft, while the cyclone is provided with control-value. This paved way for the investigation of cyclone-control-value effect on the machine's performance, to which past researchers did not pay attention.

The plantain pulps remain in the milling chamber until their particles are small enough to go through the screen. The screen was placed at 180° across the bottom of the milling chamber for easy replacement and to allow operator to turn it in order to expose new sharp edges. The passage and discharge of flour through the screen was assisted by a suction-fan, which was attached to the main shaft of the pulverizer. The fan helped air to flow through the screen of the pulverizer so as to improve its operations; prevent the screen from blinding or blocking; prevent heat buildup within the pulverizer; increase the capac-

ity of the pulverizer; and provide dust control for the pulverizer. The degree of fineness of the flour obtained is controlled by the rotor's speed, number of beaters and size of holes on the screen. According to Agriculture Canada (2012), the relations to derive a fine and coarse end products are given by Equations (1) and (2) respectively.

$$\text{Fine end product} = \text{Fast shaft speed} + \text{Small screen hole} + \text{Large number of hammers} \quad (1)$$

$$\text{Coarse end product} = \text{Slower shaft} + \text{Large screen hole} + \text{Fewer number of hammers} \quad (2)$$

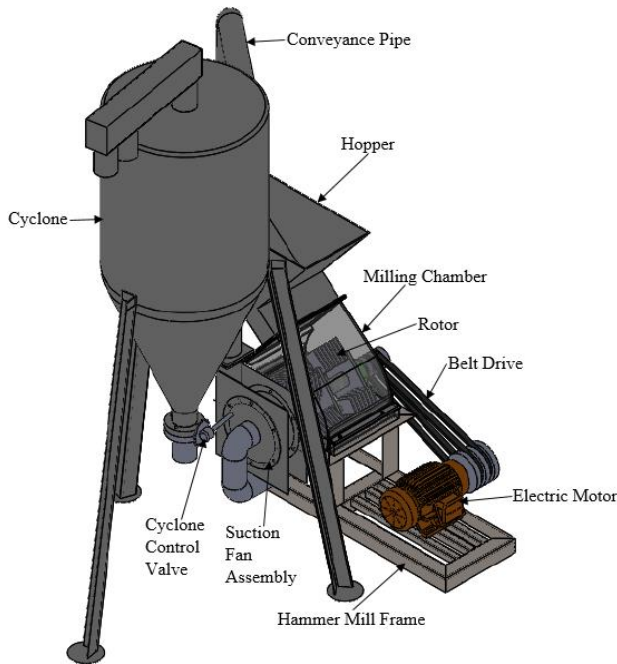


Fig. 1. Isometric view of the pulverizer

### 3.2. Design analysis of the pulverizer

Swinging hammers were selected for the pulverizer in order to prevent the rotor or hammers from becoming stocked within the plantain pulps, and for easy replacement and reusability. Thus, if one end of a beater is worn-out, the other end can be used (Ajaka and Adesina, 2014). The hammers were separated by spacers, which are round pipes of 20mm outside diameter, 12.1 mm inside diameter and length 10mm. For optimum grinding performance, longevity and to reduce centrifugal force, beaters of width 50 mm, length 75 mm and thickness 4mm were selected. Each beater has 12.1 mm drilled hole on one of its ends and all the hammers were of the same weight as suggested by Mitchell and Mwanza (2005), Agriculture Canada (2012), Dey *et al.* (2013) and Bliss (2017). Fig. 2 shows the geometry and dimensions of each beater.

Stainless steel sheet of thickness 4mm was selected for the pulverizer's housing and hopper so as to eliminate food contamination and minimize vibration.

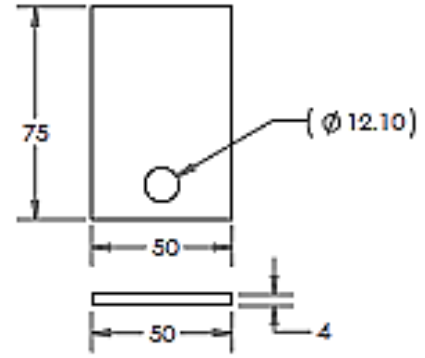


Fig. 2. Beater geometry and dimensions

Based on the recommendations of Kock (2002), Agriculture Canada (2012) and Bliss (2017), a rotor's diameter of 251.6 mm (measured from hammer tip to hammer tip), a rotor's speed of 2920 rpm; a screen area of 105600 mm<sup>2</sup> (that is, a rectangular screen of length 400 mm and width 264 mm) and twelve (12) beaters for every one horse power were selected for the pulverizer for 24 hours operation per day. A clearance of 1 mm between the beater tips and the screen was selected. Each hammer mounting plate is a square plate of length 150 mm and thickness 10 mm. The pitch circle diameter (PCD) on the mounting plate was selected to be 125.8 mm based on the selected rotor's diameter and hammer's length. The diameter of each hammer mounting rod is 12mm.

The screen diameter was determined as 253.6 mm by using Equation (3), through which an inside or internal diameter of 365.6 mm was selected for the milling chamber. Hence, the internal and external widths of the milling chamber were determined as 264 mm and 272 mm using Equation (4) and (5) respectively.

$$D_{screen} = D_{rotor} + (2 \times d_{ht,screen}) \quad (3)$$

$$W_{imc} = (t_{beater} \times N_{bpr}) + (L_{spacer} \times N_{spr}) + (N_{mplate} \times t_{mplate}) + (2 \times C_{rmp}) \quad (4)$$

$$W_{Exmc} = W_{imc} + (2 \times t_{mc}) \quad (5)$$

The length of the main shaft and the length of each hammer mounting rod were determined as 542 mm and 260 mm using Equation (6) and (7) respectively.

$$L_{MS} = W_{Exmc} + L_{pulley} + (2 \times B_w) + L_{fs} \quad (6)$$

$$L_{hr} = W_{imc} - (2 \times C_{rmp}) \quad (7)$$

Where:  $W_{imc}$  is the internal width of milling chamber;  $t_{beater}$  is beater's thickness, which is 4 mm;  $N_{bpr}$  is the number of beaters per rod, which is 15;  $L_{spacer}$  is the length of spacer, which is 10 mm;  $N_{spr}$  is the number of spacers per rod, which is 17;  $N_{rplate}$  is the number of rod plates, which is 3;  $t_{rplate}$  is the thickness of rod plate, which is 10 mm;  $C_{rmp}$  is the clearance between rod mounting plates and milling chamber, which is 2 mm;  $W_{Exmc}$  is the external width of milling chamber;  $t_{mc}$

is the thickness of milling chamber, which is 4 mm;  $L_{MS}$  is the length of main shaft;  $L_{pulley}$  is the length of pulley, which is 100 mm;  $B_w$  is the bearing width, which is 50 mm;  $L_{fs}$  is the length of fan shaft, which is 70 mm;  $D_{screen}$  is the screen diameter;  $d_{ht,screen}$  is the distance between hammer tips and screen, which is 1 mm; and  $L_{hr}$  is the length of each hammer rod.

### 3.2.1. Design of pulverizer hopper

The hopper is a stainless steel structure, which is a hollow frustum of a rectangular-based pyramid as shown in Fig. 3. The hopper is made of stainless steel sheet of thickness 3 mm. According to CEMC (2012), the volume of the hopper ( $V_{mh}$ ) was estimated to be 33661951.2 mm<sup>3</sup> using Equation (8).

$$V_{mh} = \left\{ (A \times B) + (C \times D) + \sqrt{(A \times B) + (C \times D)} \right\} \frac{H}{3} \quad (8)$$

Where: H is the height of the pulverizer hopper, which is 500 mm; A is the length of the hopper's top, which is 600 mm; B is the width of the hopper's top, which is 230 mm; C is the length of the hopper's bottom, which is 230 mm; and D is the width of the hopper's bottom, which is 230 mm.

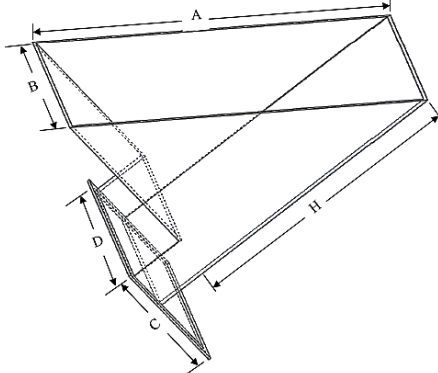


Fig. 3. Pulverizer hopper

### 3.2.2. Design of belt drive for the pulverizer

The Speed ratio of the belt drive was determined to be 2 using Equation (9) and design power ( $P_D$ ) for the belt drive was obtained as 5.968 kW from Equation (10) by selecting a Service Factor (SF) of 1.6 for the pulverizer (Fenner, 2009). Thus, a belt of SPZ or QXPZ cross section was chosen. After establishing a minimum pitch diameter of 67 mm for the pulleys, pulleys of 160 mm and 80 mm pitch diameters were selected (from Centre distance tables for SPZ and QXPZ cross section wedge-belts) for the electric motor and rotor's main shaft respectively.

$$SR_{mill} = N_{rsp}/N_{mp} \quad (9)$$

$$P_D = P_m \times SF \quad (10)$$

Where:  $SR_{mill}$  is the speed ratio of rotors' pulley to electric motor's pulley;  $N_{rsp}$  is the rotational speed of the rotors' shaft pulley; and  $N_{mp}$  is the speed of electric motor's pulley.

According to Childs (2004), Fenner (2009) and Udo *et al.* (2015), the minimum and maximum centre distances of the two pulleys were estimated to be 140 mm and 480 mm using Equation (11) and (12) respectively. It was ensured that the centre distance selected was greater than the diameter of the larger pulley as recommended. Hence, a center distance of 435 mm, which satisfied Equation (14), was selected in order to balance the weight of the pulverizer; a corresponding correction factor of 0.95 was also selected; while the belt length,  $L_B$ , was obtained as 1251 mm by using Equation (15). Moreover, the power rating per belt, corrected power per belt and number of belts required to drive the pulverizer's rotor were calculated as 3.69 kW, 3.51 kW and 2 by using Equation (16), (17) and (18) respectively. From Power Ratings and Additional Power Ratings tables for SPZ belt Section, rated power per belt was estimated to be 3.235 kW; while additional power was estimated to be 0.45 kW.

$$C_{d,min} = 0.55(D_{rsp} + D_{mp}) + t_{belt} \quad (11)$$

$$C_{d,max} = 2(D_{rsp} + D_{mp}) \quad (12)$$

$$C_{d,ave} = \frac{C_{d,min} + C_{d,max}}{2} = 310 \text{ mm} \quad (13)$$

$$\begin{cases} C_{d,min} \leq C_d \leq C_{d,max} \\ C_d \text{ must be } > D_{mp} \end{cases} \quad (14)$$

$$L_B = 2C_d + \frac{(D_{mp} - D_{rsp})^2}{4C_d} + \frac{\pi(D_{mp} + D_{rsp})}{2} \quad (15)$$

Power rating per belt = Rated power + Additional power (16)

Corrected Power per belt = Power rating per belt × Correction Factor (17)

$$\text{Number of belts required} = \frac{\text{Design Power}}{\text{Corrected Power per belt}} \quad (18)$$

Where:  $D_{rsp}$  is the diameter of rotor's shaft pulley;  $D_{mp}$  is the diameter of electric motor pulley;  $C_d$  is the selected center distance;  $t_{belt}$  is the belt thickness, which is 8 mm;  $C_{d,min}$ ,  $C_{d,max}$  and  $C_{d,ave}$  are the minimum, maximum and average center distances between the two pulleys respectively.

### 3.2.3. Design of the main shaft for the pulverizer

The twisting moment or torque transmitted by the shaft was calculated as 13.2 Nm using Equation (19). The loading of the main shaft was treated as a simply supported beam with uniformly distributed load, converted to point load, in-between two bearing supports with an overhang load on each side of the bearing supports as shown in Fig. 4, 5 and 6. The total weight, which is the point load, acting at the middle of the rotor's shaft in-between the two bearing supports is 154 N. This is a combination of beaters' total weight, total weight of beaters' mounting rods, total weight of beaters' mounting plates and total weight of spacers. The weight of the suction-fan assembly for the pulverizer,  $F_{SF}$ , is 18 N, while pulley weight is 18 N.

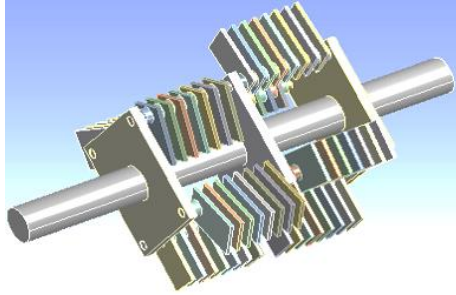


Fig. 4. Isometric view of rotor's assembly for the pulverizer

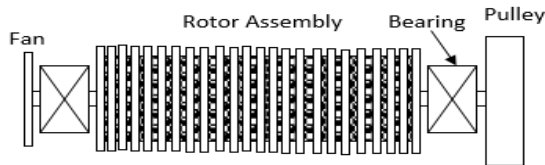


Fig. 5. Space diagram of fan, bearing, rotor and pulley assembly for the pulverizer

$$T_{tms} = (T_{ts} - T_{ss})R_{rsP} = \frac{60P_{sm}}{2\pi N_{rp}} \quad (19)$$

$$V_{rsp} = (\pi \times D_{rsP} \times N_{rp})/60 = 11.3112 \text{ m/s} \quad (20)$$

$$T_{ts}/T_{ss} = 10^{\mu\theta/2.3 \sin \beta} \quad (21)$$

Substituting Equation (21) into Equation (19) gives Equation (22).

$$T_{ss} = T_{tms} / \{R_{rsP}(10^{\mu\theta/2.3 \sin \beta} - 1)\} \quad (22)$$

$$\alpha = (D_{mp} - D_{rsP})/2C_d \approx 0.092 \text{ rad} \quad (23)$$

$$\theta = (\pi - 2\alpha) \approx 2.96 \text{ radians} \quad (24)$$

$$\mu = 0.54 - [42.6/(152.6 + V_{rsp})] = 0.28 \quad (25)$$

$$\therefore T_{ss} \approx 22.2 \text{ N}$$

From Equation (21),  $T_{ts} = T_{ss} \times 10^{\mu\theta/2.3 \sin \beta} \approx 351.9 \text{ N}$

$$F_{rsp} = T_{ts} + T_{ss} + W_{rsp} = 392.1 \text{ N}$$

Summing all the vertical forces or loads on the rotor's assembly gives

$$R_1 + R_2 = 18 + 154 + 392.1 = 564.1 \text{ N}$$

Taking moments about  $R_2$ , we have  $272R_1 + (392.1 \times 154) = (388 \times 18) + (136 \times 154)$

$$\therefore R_1 = -119.32 \text{ N. Hence, } R_2 = 564.1 - R_1 = 683.42 \text{ N}$$

The maximum bending moment (BM) was obtained at point  $R_2$  as follows:

$$\text{BM to the right, } BM_{R_2} = 154F_{rsp} = 154 \times 392.1 = 60383.4 \text{ Nmm or } 60.3834 \text{ Nm}$$

$$\text{BM to the left, } BM_{R_2} = (18 \times 388) - 119.23 \times 272 + (154 \times 136) = 60383.04 \text{ Nmm}$$

The maximum bending moment  $M_{ms}$  is 60.38304 Nm. The diameter of the shaft was then obtained as 25 mm using Equation (26) (Khurmi and Gupta, 2008). Hence, a shaft of 30 mm diameter was selected for the pulverizer.

$$d_{ms} = \sqrt[3]{\frac{16(\sqrt{(K_m \times M_{ms})^2 + (K_t \times T_{tms})^2})}{\pi \times \tau_{ms}}} \quad (26)$$

Where:  $T_{tms}$  is the twisting moment of or torque transmitted by the shaft (in Nm);  $T_{ts}$  is the tight side tension;  $T_{ss}$  is the slack side tension;  $R_{rsP}$  is the radius of rotor's shaft pulley;  $P_{sm}$  is the selected motor power or power transmitted by shaft (in watts), which is 3730 watts;  $N_{rsp}$  is the speed of rotor's shaft pulley, which is 2700 rpm;  $\mu$  is the coefficient of friction between belt and pulley;  $V_{rsp}$  is the velocity of the rotor's shaft pulley;  $\theta$  is the angle of lap or contact between belt and pulley;  $b$  is half the groove angle of the pulley, which is  $17.5^\circ$ ;  $d_{ms}$  is the main shaft diameter;  $M_{ms}$ ,  $T_{tms}$  and  $\tau_{ms}$  are the maximum bending moment, twisting moment and allowable shear stress of the main shaft (which is 42 MPa) respectively.

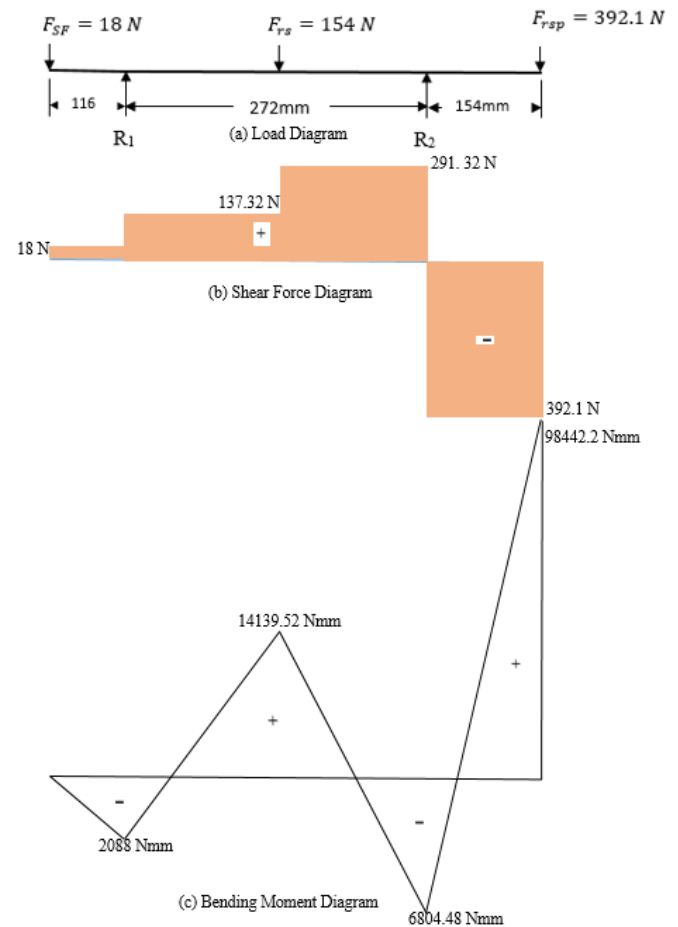


Fig. 6. Load, shear force and bending moment diagrams of the rotor's assembly

## 4. Results and discussion

### 4.1. Simulation and performance evaluation of the pulverizer

Using ANSYS Mechanical of ANSYS 14.0 software, static analysis of the pulverizer's finite element model (FEM) was done in order to ascertain its workability and structural integrity before fabrication as suggested by Olutomilola (2021). It

was assumed that forces or loads applied were evenly distributed on the machine's members. The simulation of the pulverizer frame showed a maximum stress of 1.514 MPa, a maximum deformation of  $6.73 \times 10^{-6}$  mm and a maximum strain of  $7.5715 \times 10^{-6}$  uniformly distributed at the flange, on which the machine is seated, when subjected to a load of 700 N as shown in Fig. 7, 8 and 9 respectively. The FEA conducted on the pulverizer rotor or beater assembly showed a maximum stress of 7.0259 MPa and a maximum deformation of  $5.6274 \times 10^{-5}$  mm experienced at some points when subjected to a load of 400 N and a torque of 20 Nm as shown in Fig. 10 and 11 respectively.

However, the maximum stress values obtained from the FEA of the frame and rotor were observed to be far below the yield strength values of the mild steel (248.2 MPa) and stainless steel (172.3 MPa) materials selected for their fabrication as shown in Fig. 7 and 10 respectively. The pulverizer was then fabricated as shown in Fig. 12. The performance of the pulverizer was then evaluated with the following results: a throughput of 400 kg/h, specific rate of breakage of 0.96, crushing efficiency of 96% and mass loss of 4% were obtained by using Equation (27), (28), (29) and (30) respectively.

$$Q_{tp} = M_o / t_g \quad (27)$$

$$B_{srb} = M_o / M_i \quad (28)$$

$$C_{eff} = (M_o / M_i) \times 100\% \quad (29)$$

$$M_{pL} = \{(M_i - M_o) / M_i\} \times 100\% \quad (30)$$

Where:  $Q_{tp}$  is the throughput of the pulverizer in kg/h;  $M_o$  is the output mass (i.e. the quantity of plantain flour that passed through the screen in kg), which is approximately equal to 4.8 kg;  $t_g$  is the time taken to get the output mass in hour;  $B_{srb}$  is the specific rate of breakage;  $M_i$  is the input mass in kg, which is 5 kg;  $C_{eff}$  is the crushing efficiency of the pulverizer; and  $M_{pL}$  is the percentage of lost mass (Probst et al., 2013; Mohamed et al., 2015).

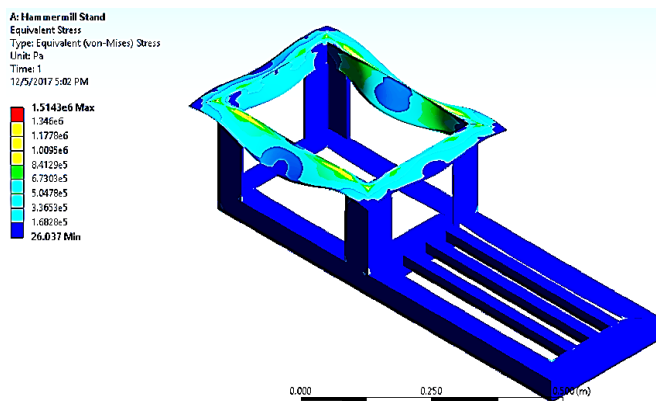


Fig. 7. Stress distribution within the machine frame

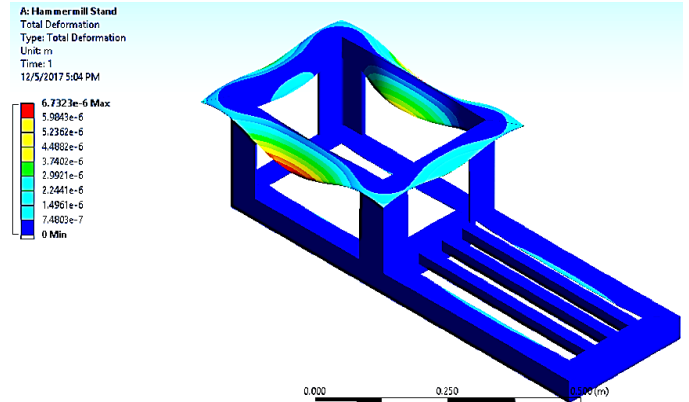


Fig. 8. FEM of deformation of the machine frame

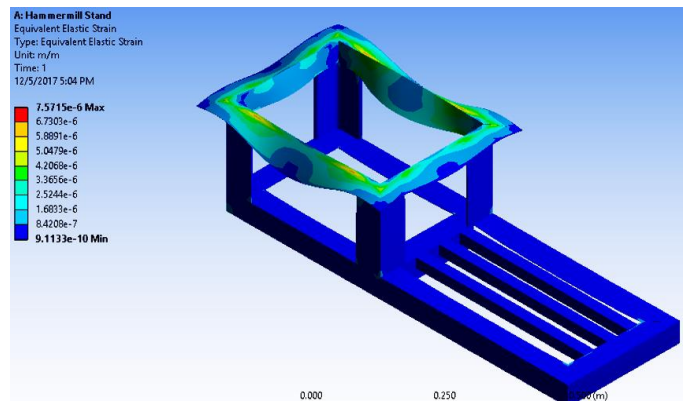


Fig. 9. Strain distribution within the machine frame

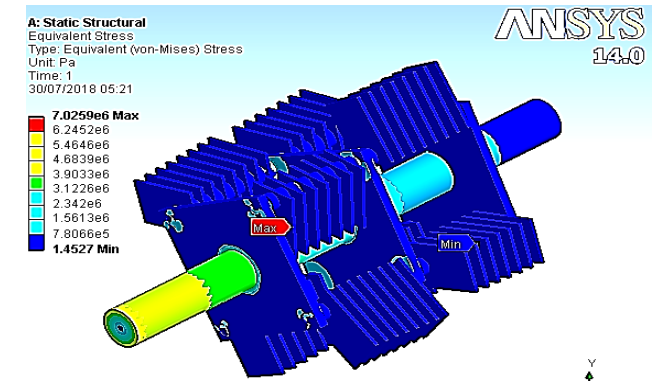


Fig. 10. FEM of stress distribution within the rotor

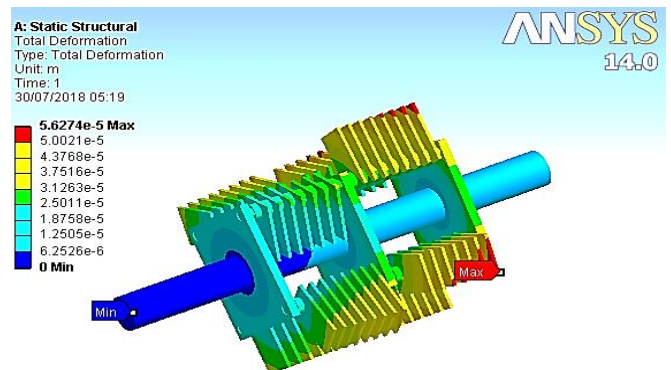


Fig. 11. FEM of deformation distribution within the rotor



Fig. 12. The fabricated pulverizer

#### 4.2. Test of control-valve effect on flour conveyance

The effect of cyclone control-valve on flour conveyance and the pulverizer efficiency was evaluated by pulverizing 1 kg of dry plantain pulps for each of the following control-valve positions: completely closed, partially opened and fully opened. The pulverizer was allowed to run for one minute in each case. It was observed that only 100 g of flour were delivered into the cyclone when the control-valve was fully closed. Also, 875 g and 900 g of flour were delivered into the cyclone when the control-valve was half opened and fully opened respectively as shown in Table 1.

Table 1. Effect of control-valve on flour conveyance

S/N	Control-valve Position	Input Weight (g)	Time (Sec-onds)	Output Weight (g)
1	Fully Closed	1000	60	100
2	Half Opened	1000	60	875
3	Fully Opened	1000	60	900

#### 4.3. Particle size distribution and analysis of the plantain flour obtained

The particle size of the flour obtained from the pulverizer was examined. The particle size distribution of the flour was then determined using sieving method by employing sieve vibrator equipment. Five available sieve sizes (600 $\mu$ m, 500 $\mu$ m, 250 $\mu$ m, 210 $\mu$ m and 180 $\mu$ m) were mounted on the sieve vibrator in decreasing order with a pan collector directly placed beneath sieve 180 $\mu$ m as shown in Fig. 13. Then, 500 g of the flour was introduced into the tier of sieves and the sieve vibrator was operated for 25 minutes. The results obtained are as presented in Table 2. The percentage mass retained on each sieve was then determined by using Equation (32) as shown in Table 3. Particle size analysis was then carried out on the flour in order to determine its average particle size using Equation (31), (32) and (33). The results obtained are as presented in

Table 3. The average particle size of the flour obtained was 236 $\mu$ m.

Moreover, the particle size of the plantain flour obtained from the pulverizer is not expected to be greater than 500 $\mu$ m, which is the size of the screen used in its milling chamber. Thus Table 3 shows that 11.9 and 8.36 grams of the flour were retained by 600 $\mu$ m and 500 $\mu$ m sieve sizes respectively as oversize during sieving. This made the total mass of oversized flour particles obtained to be 20.26 grams. Hence, the efficiency of the pulverizer, based on the required particle size, was obtained as 96% using Equation (34).

Table 2. Particle size distribution in descending order

S/N	Sieve Size ( $\mu$ m)	Mass Retained (g)
1	600	11.90
2	500	8.36
3	250	431.21
4	210	10.76
5	180	13.74
6	Pan Collector	23.48
TOTAL		499.45

Table 3. Particle size analysis of the plantain flour obtained

S/N	Sieve Size ( $\mu$ m)	Average Sieve Size ( $\mu$ m)	MR (g)	PMR (%)	PMD ( $\mu$ m)
1	180	90	13.74	2.9	261
2	210	195	10.76	2.3	448.5
3	250	230	431.21	90.6	20838
4	500	375	8.36	1.8	675
5	600	550	11.90	2.5	1375
TOTAL			475.97	100	23597.5

$$ASS = (D_1 + D_2)/2 \quad (31)$$

$$PMR = (MR/TMR) \times 100\% \quad (32)$$

$$MMD = (\sum_{i=1}^5 PMD) / (\sum_{i=1}^5 PMR) \approx 236 \mu\text{m} \quad (33)$$

$$\eta_{bps} = \frac{TMS - MOS}{TMS} \times 100\% \approx 96\% \quad (34)$$

Where: ASS is the average sieve size; PMR is the percentage mass retained; MR is the mass retained; TMR is the total mass retained, which is 475.97 g; MMD is the mass mean diameter (which is the average particle size of the plantain flour); PMD is the particle mean diameter;  $\eta_{bps}$  is the efficiency of the pulverizer based on the required particle size; TMS is the total mass sieved, which is 500 g; and MOS is the mass of oversized flour (Sonaye and Baxi, 2012).



Fig. 13. (a) Sieve vibrator (b) Sieves with retained plantain flour

#### 4.4. Discussion of evaluation results

It is to be noted that the maximum stress values obtained (1.514 MPa and 7.0259 MPa) are far lower than the yield strength values of the mild steel (248.2 MPa) and stainless steel (172.4 MPa) selected for the frame and rotor respectively. This is an indication that the machine will be able to serve its intended purpose without failure, which is an attestation to the machine's fitness for fabrication. However, the points where induced stresses are maximum on the frame and rotor were keenly considered during fabrication, since they are locations where structural failure may likely be initiated after a long period in service.

It was also observed from the fabricated machine's evaluation that the efficiency of the fan, screen and rotor can significantly be influenced by the position of the cyclone's control-valve. This efficiency was also found to be inversely proportional to the feed rate. Since only 100 g of flour were delivered into the cyclone when the control-valve was fully closed as shown in Table 1. This means that major or larger part of the flour remained within the pulverizer. The implication of this is that, continuous feeding of the pulverizer while the control-valve is fully closed will lead to blockage of flour passage, blockage of the screen, eventual backflow of material, wastage of material and reduced machine efficiency due to generation of back-pressure within the cyclone. Hence, the control-valve should always be opened completely while milling operation is ongoing so as to avoid the aforementioned problems. Opening the control-valve during operation will help the pulverizer perform without any problem.

Table 3 shows 2.9%, 2.3%, 90.6%, 1.8% and 2.5% of the total flour introduced into the tier of sieves being retained by the screens of 180  $\mu\text{m}$ , 210  $\mu\text{m}$ , 250  $\mu\text{m}$ , 500  $\mu\text{m}$  and 600  $\mu\text{m}$  sieves respectively. Thus, the greatest proportion of the plantain flour was retained on the screen of 250 $\mu\text{m}$  sieve size during the particle size analysis. It can, thus, be inferred from the particle size analysis conducted on the flour obtained that the average particle size of flour obtainable from the pulverizer at any time is 0.236 mm. This shows conformity with standardized particle size of plantain flour. Also, the 96% efficiency obtained, based on particle size distribution, is an indication that the pulverizer will be able to effectively pulverize dry plantain pulps into flour of 236 $\mu\text{m}$  particle size whenever a screen size of 500  $\mu\text{m}$  is used in its milling chamber.

#### 5. Summary and conclusion

In this study, consumption of plantain and its products as a promising way to defeat COVID-19 among diabetic patients was established via researchers' works (Olutomilola, 2021). This attests to the relevance of this study in this critical period in the history of the world. A pulverizer, with an efficiency of 96% and a throughput of 400 kg/h, was developed for a plant that processes unripe plantain into flour and its performance evaluated. The average particle size of plantain flour obtained was 236  $\mu\text{m}$  by using a screen size of 500  $\mu\text{m}$ . As revealed by the results obtained during its performance evaluation, the control-valve of the pulverizer's cyclone had significant influence on the machine's efficiency. It can be said that partial or

full closure of the control-valve would lead to lots of technical problems that are capable of adversely affecting the pulverizer's overall efficiency/performance. Thus, leaving the control-valve fully opened, during operation, would help the pulverizer perform effectively. It can, therefore, be inferred that the pulverizer is able to serve its intended purpose in the process plant as it was able to pulverize, sieve and convey material to the next processing stage during evaluation.

This study has been able to establish that cyclone control-valve can significantly affect pulverizer's flour conveyance and overall performance, which other researchers failed to do (Olutomilola, 2019). However, the experiment for evaluating control-valve effect on the pulverizer's overall efficiency will be repeated for about nine more times in subsequent research for result accuracy/validation and the principle behind this phenomena will be investigated. This would be followed by full automation and incorporation of the pulverizer into the plantain flour production and packaging plant.

#### Acknowledgements

The authors wish to acknowledge Tertiary Education Trust Fund (TETFund) Nigeria for financially supporting this study, under research grant Ref: VCPU/TETFund/155. Advanced Manufacturing and Applied Ergonomics Research Team (AMAERT), Engr. Adebola Adesina, Dr. B. O. Akinnuli, Dr. O. Z. Ayodeji, Dr. O. M. Olabanji, Emmanuel Olufemi Oyelami and Waheed Ayodeji Oyewole are also appreciated for their contributions towards the success of this work.

#### Reference

- Adekomaya, S.O., Samuel, O.D., 2014. Design and development of a petrol-powered hammer mill for rural nigerian farmers. *Journal of Technologies and Policy*, 4(4), 65-74.
- Adetola, S.O., Oyejide, A.J., 2015. Development of a bone milling machine with safety hollow and low risk of electrical damage. *International Journal of Modern Engineering Research*, 5(6), 52-59, [https://ia801303.us.archive.org/33/items/Httpijmer.compapersVol5\\_Issue6Version-1G0506\\_01-5259.pdf/G0506\\_01-5259.pdf](https://ia801303.us.archive.org/33/items/Httpijmer.compapersVol5_Issue6Version-1G0506_01-5259.pdf/G0506_01-5259.pdf)
- Adeyeri, M.K., Ayodeji, S.P., Olutomilola, E.O., Bako J.O., 2020. Design of a screw conveyor for transporting and cooling plantain flour in a process plant. *Jordan Journal of Mechanical and Industrial Engineering*, 14(4), 425-436, <http://jjmie.hu.edu.jo/vol14-4/08-38-20.pdf>
- Agriculture Canada, 2012. Handling agricultural materials: Size Reduction and Mixing, Digitized Ed. Canadian Government Publishing Centre, Minister of Supply and Services, Ottawa, Canada. Retrieved from <https://archive.org/details/handlingagri00bire>
- Ajaka, E.O., Adesina, A., 2014. Design, fabrication and testing of a laboratory size hammer mill. *International Journal of Engineering and Advance Technology Studies*, 2(2), 11-21, <http://www.eajournals.org/wp-content/uploads/Design-Fabrication-and-Testing-Of-a-Laboratory-Size-Hammer-Mill1.pdf>
- Ajiboye, B.O., Oloyede, H.O.B., Salawu, M.O., Antihyperglycemic and antidiabetic activity of Musa paradisiaca-based diet in alloxan-induced diabetic rats, *Food Science and Nutrition*, 6, 137-145, DOI: 10.1002/fsn3.538.
- Alonso-Gomez, L.A., Solarte-Toro, J.C., Bello-Perez, L.A., Cardona-Alzate, C.A., 2020. Performance evaluation and economic analysis of the bioethanol and flour production using rejected unripe plantain fruits (*Musa paradisiaca* L.) as raw material. *Food and Bioproducts Processing*, 121, 29-42, DOI: 10.1016/j.fbp.2020.01.005.
- Ayodeji, S.P., 2016. Conceptual design of a process plant for the production of plantain flour. *Cogent Engineering*, 3, 1-16, DOI: 10.1080/23311916.2016.1191743.



- Bliss, 2017. "Hammermill," Bliss Industries Inc., Ponca City, Oklahoma USA. Retrieved from <http://www.bliss-industries.com> (Accessed 27/06/2017).
- CEMC, 2012. Screw conveyor components and design, version 2.20. Screw Conveyor Manual, Conveyor Engineering and Manufacturing Co. (CEMC). Retrieved from [www.conveyoreng.com](http://www.conveyoreng.com)
- Childs, P.R.N., 2004. Mechanical Design (2nd Ed.). Oxford, UK: Elsevier Butterworth-Heinemann, 154-175.
- Dey, S.K., Dey, S., Das, A., 2013. Comminution features in an impact hammer mill. Powder Technology, 235, 914-920, DOI: 10.1016/j.powtec.2012.12.003.
- Ebunilo, P.O., Obanor, A.I., Ariavie, G.O., 2010. Design and preliminary testing of a hammer mill with end-suction lift capability suitable for commercial processing of grains and solid minerals in Nigeria. International Journal of Engineering Science and Technology, 2(6), 1581-1593.
- Fenchea, M., 2012. Design of hammer mills for optimum performance. Journal of Vibration and Control, 19(14), 2100-2108, DOI: 10.1177/1077546312455210.
- Fenner, 2009. Drive design and maintenance manual. ERIKS Industrial Services Limited. Retrieved from [www.fptgroup.com](http://www.fptgroup.com)
- Hadi, M.I., Bawa, M.A., Dandakouta, H., Ahmed, M., Kamtu, P.M., 2017. Improvement on the design, construction and testing of hammer mill. American Journal of Engineering Research, 6(3), 139-146, [http://www.ajer.org/papers/v6\(03\)/X0603139146.pdf](http://www.ajer.org/papers/v6(03)/X0603139146.pdf)
- Hussain, A., Bhowmik, B., Moreira, N.C.D.V., 2020. COVID-19 and diabetes: knowledge in progress. Diabetes Research and Clinical Practice: 108142, 162, 1-9, DOI: 10.1016/j.diabres.2020.108142.
- Jibrin, M.U., Amoye, M.C., Akonyi, N.S., Oyeleran, O.A., 2013. Design and development of a crop residue crushing machine. International Journal of Engineering Inventions, 2(8), 28-34, <http://www.ijejournal.com/papers/v2i8/D02082834.pdf>
- Khurmi, R.S., Gupta, J.K., 2008. A Textbook of Machine Design, first multicolour ed. Eurasia Publishing House (PVT.) Ltd., Ram Nagar, New Delhi, India, 470-557, 677-739, 820-879.
- Koch, K., 2002. Hammermills and Roller Mills. Department of Grain Science, Kansas State University, Agricultural Experiment Station and Cooperative Extension Service, 1-5. Retrieved from [www.oznet.ksu.edu/grsiext](http://www.oznet.ksu.edu/grsiext)
- Mitchell, C.J., Mwanza, M., 2005. Farmlime Manual for Small-scale Production of Agricultural Lime. British Geological Survey, Economic Minerals Programme, Commissioned Report CR/05/092N. Retrieved from <http://www.mineralsuk.com/britmin/farmlime.pdf>
- Mohamed, T.H., Radwan, H.A., Elashhab, A.O., Adly, M.Y., 2015. Design and evaluation of a small hammer mill. Egyptian Journal of Agricultural Research, 93(5B), 481-495.
- Morris, K.J., Kamarulzaman, N.H., Morris, K.I., 2019. Small-scale postharvest practices among plantain farmers and traders: A potential for reducing losses in rivers state. Nigeria. Scientific African, 4, 1-10, DOI: 10.1016/j.sciaf.2019.e00086.
- Nasir, A., 2005. Development and testing of a hammer mill. Assumption University Journal of Technology, 8(3), 124-130.
- Ogedegbe, T.I., Abadariki, O.D., 2014. Development and performance evaluation of a bone-milling cum pulverizing machine. The West Indian Journal of Engineering, 37(1), 23-28. [http://sta.uwi.edu/eng/wije/vol3701\\_jul2014/documents/Vol37No1ManTIOgedegbeJul2014.pdf](http://sta.uwi.edu/eng/wije/vol3701_jul2014/documents/Vol37No1ManTIOgedegbeJul2014.pdf)
- Olutomilola, E.O., 2019. Development of a process plant for plantain flour production. A PhD Thesis in Mechanical Engineering Department, School of Engineering and Engineering Technology, Federal University of Technology, Akure, Ondo State, Nigeria.
- Olutomilola, E.O., 2021. A review of raw plantain size reduction. Scientific African, 12, 1-15, DOI: 10.1016/j.sciaf.2021.e00773.
- Olutomilola, E.O., Ayodeji, S.P., Adeyeri, M.K., 2019. Finite element analysis of a washing and preheating unit designed for plantain flour process plant. International Journal of Engineering Technologies, 5(4), 117-127, <https://dergipark.org.tr/en/pub/ijet/issue/53836/560389>
- Olutomilola, E.O., Ayodeji, S.P., Adeyeri, M.K., 2020. Design and structural analysis of a particulating machine for plantain flour process plant. ARPN Journal of Engineering and Applied Sciences, 15(17), 1816-1824, [http://www.arpnjournals.org/jeas/research\\_papers/rp\\_2020/jeas\\_0920\\_8\\_295.pdf](http://www.arpnjournals.org/jeas/research_papers/rp_2020/jeas_0920_8_295.pdf)
- Olutomilola, E.O., Ayodeji, S.P., Adeyeri, M.K., 2021. Design and Finite Element Analysis of Flour Packaging Machine for Plantain Processing Plant. Mindanao Journal of Science and Technology, 19(1), 269-292, <https://mjst.ustp.edu.ph/index.php/mjst/article/view/784/184>
- Olutomilola, E.O., Omoaka, A., 2018. Theoretical design of a plantain peeling machine. FUTA Journal of Engineering and Engineering Technology, 12(2), 229-237, <https://www.futa.edu.ng/journal/home/volumep/53/12>
- Oluwajuyitan, T.D., Ijarotimi, O.S., 2019. Nutritional, antioxidant, glycaemic index and antihyperglycaemic properties of improved traditional plantain-based (Musa AAB) dough meal enriched with tigernut (Cyperus esculentus) and defatted soybean (Glycine max) Flour for diabetic patients. Heliyon, 5, 1-27, DOI: 10.1016/j.heliyon.2019.e01504.
- Probst, K.V., Ambrose, R.P.K., Pinto, R.L., Bali, R., Krishnakumar, P., Ileleji, K.E., 2013. The effect of moisture content on the grinding performance of corn and corncobs by hammermilling. American Society of Agricultural and Biological Engineers, 56(3), 1025-1033, <https://core.ac.uk/download/pdf/18529159.pdf>
- Seewoodhary, J., Oozageer, R., 2020. Coronavirus and diabetes: an update. Practical Diabetes, 37(2), 41-42, DOI: 10.1002/pdi.2260.
- Sonaye, S.Y., Baxi, R.N., 2012. Particle size measurement and analysis of flour. International Journal of Engineering Research and Applications, 2(3), 1839-1842, [http://www.ijera.com/papers/Vol2\\_issue3/KZ2318391842.pdf](http://www.ijera.com/papers/Vol2_issue3/KZ2318391842.pdf)
- Udo, S.B., Adisa, A.F., Ismaila, S.O., Adejuyigbe S.B., 2015. Development of palm kernel nut cracking machine for rural use. Agricultural Engineering International: CIGR Journal, 17(4): 379-388, <https://cigrjournal.org/index.php/Ejournal/article/view/3417/2270>
- Wang, A., Zhao, W., Xu, Z., Gu, J., 2020. Timely blood glucose management for the outbreak of 2019 novel coronavirus disease (COVID-19) is urgently needed. Diabetes Research and Clinical Practice, Elsevier 108118; 162, 1-2, DOI: 10.1016/j.diabres.2020.108118.

## 车前草粉加工厂粉碎机的研制及性能评价

### 關鍵詞

糖尿病 COVID-19  
粉碎机开发  
绩效评估  
芭蕉  
面粉加工厂

### 摘要

糖尿病被判定为 2019 年冠状病毒传染病 (COVID-19) 的危险因素, 可以通过食用车前草及其相关产品来控制。由于其保质期很短, 车前草通常被加工成面粉和其他可储存/增值的产品。要将未成熟的大蕉果肉加工成面粉, 需要在干燥后缩小尺寸。本文介绍了一种粉碎、筛分和将材料输送到大蕉面粉加工厂的下一个加工阶段的粉碎装置的开发和性能评估。它的模型是使用 solidworks 应用软件开发。在设计分析之后, 对模型进行模拟以确定其制造的适用性/充分性。粉碎机是使用当地可用的材料制造的。其性能评估给出了 400kg/h 的吞吐量、96% 的破碎效率和 96% 的效率 (基于所需的粒度)。使用 500  $\mu\text{m}$  筛网获得的面粉的平均粒度为 236  $\mu\text{m}$ 。还通过在阀门完全关闭、部分关闭和完全打开时允许其运行来研究旋风控制阀对粉碎机整体效率的影响。据观察, 控制阀的位置显著影响了机器的性能/效率。因此可以推断旋风控制阀的位置对粉碎机的效率/性能有显著影响。因此, 在操作期间保持控制阀完全打开将有助于粉碎机以最佳效率运行, 因为粉碎机能够在该位置有效地将材料输送到性能评估期间的下一个加工阶段。